

# TOWARDS END-TO-END SPEAKER DIARIZATION IN THE WILD

Zexu Pan<sup>1,2</sup>, Gordon Wichern<sup>1</sup>, François G. Germain<sup>1</sup>, Aswin Subramanian<sup>1</sup>, Jonathan Le Roux<sup>1</sup>

<sup>1</sup>Mitsubishi Electric Research Laboratories (MERL), Cambridge, MA, USA

<sup>2</sup>Institute of Data Science, National University of Singapore, Singapore

## ABSTRACT

Speaker diarization algorithms address the “who spoke when” problem in audio recordings. Algorithms trained end-to-end have proven superior to classical modular-cascaded systems in constrained scenarios with a small number of speakers. However, their performance for in-the-wild recordings containing more speakers with shorter utterance lengths remains to be investigated. In this paper, we address this gap, showing that an attractor-based end-to-end system can also perform remarkably well in the latter scenario when first pre-trained on a carefully-designed simulated dataset that matches the distribution of in-the-wild recordings. We also propose to use an attention mechanism to increase the network capacity in decoding more speaker attractors, and to jointly train the attractors on a speaker recognition task to improve the speaker attractor representation. Even though the model we propose is audio-only, we find it significantly outperforms both audio-only and audio-visual baselines on the AVA-AVD benchmark dataset, achieving state-of-the-art results with an absolute reduction in diarization error of 23.3%.

**Index Terms**— Speaker diarization, EEND-EDA, attention attractors, speaker recognition

## 1. INTRODUCTION

Speech is arguably the most natural form of human communication, effectively delivering rich information regarding, for example, a speaker’s emotion, identity, location, and spoken content. Such information could be obtained by machine listening algorithms [1–4]. However, those algorithms are often most effective when applied to the isolated audio segments where the speaker is active. As a result, it is beneficial to recognize “who spoke when” as a pre-processing step, i.e., the start and end times of each speaker’s utterance in a conversation, a task also known as speaker diarization.

A classical example of speaker diarization algorithm is a cascaded system of voice activity detection (VAD), frame segmentation, speaker representation extraction (SRE), and clustering [5, 6]. The speaker count is determined in the clustering step by comparing the speaker representations of every frame. Thus, errors in VAD and SRE can compound to markedly lower the speaker diarization performance. Meanwhile, such algorithms often cannot handle overlapping speakers as each frame is usually assigned to a single speaker.

End-to-end neural-network-based speaker diarization algorithms have emerged in recent years, greatly simplifying the complicated model-building and inference process of their classical counterparts, while usually performing better by directly optimizing the final metric of interest. Such algorithms also naturally handle

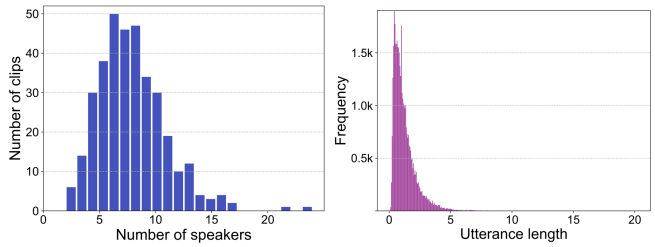


**Fig. 1.** Histograms of the number of speakers (left) and the utterance length in seconds (right) of the audio recordings in the AVA-AVD dataset, plots are taken from [12].

speaker overlap, by decoding a speech activity stream for every speaker. The number of speakers is determined either by setting an upper limit and having the network always output the maximum number of streams, such as in end-to-end neural diarization (EEND) [7], or by iteratively estimating an attractor that represents a new speaker until all speakers have been estimated and a stop flag is raised, such as in EEND with an encoder-decoder based attractor (EDA) calculation module (EEND-EDA) [8, 9]. The latter has attracted increasing attention as it can flexibly deal with an unknown number of speakers. In either case, permutation invariant training (PIT) [10, 11] is needed as there is a speaker order ambiguity between the network outputs and the ground-truth labels.

EEND-EDA was shown to perform remarkably well in meetings or conversation scenarios, namely the CALLHOME and DIHARD datasets [13], where there are rarely more than 10 people involved in a given audio recording. However, in some circumstances such as movies or in-the-wild recordings, more people may be involved, and the length of many utterances may be very short. This is exemplified by the AVA-AVD dataset [12], where as shown in Fig. 1, a 5-minute movie clip may contain up to 20 speakers, while the utterance length is typically much shorter than in meetings. Additionally, such recordings present multiple challenges that will put an end-to-end system to a stress test: i) the presence of various types of noises, sound effects, and music; ii) the stability of PIT for diarization with more speakers and shorter utterances, and its factorial complexity against the number of speakers; iii) the capacity of EDA in capturing and decoding representative attractors for all speakers.

In this work, we investigate the capability of an EEND-EDA system on the in-the-wild movie-style audio recordings from the AVA-AVD benchmark [12]. We show that EEND-EDA can be made to outperform classical cascaded systems on AVA-AVD by pre-training it on a carefully-designed simulated dataset that matches the distribution of movie-style audio recordings. We further propose an attention-based EDA module that increases network capacity when decoding a large number of speaker attractors. We also pro-

This work was performed while Zexu Pan was an intern at MERL.

pose jointly training the speaker attractors on a speaker recognition task, to further improve the attractor representation. Our final (audio-only) proposed model, which we refer to as EEND-EDA-SpkAtt, outperforms both audio-only and audio-visual baselines, and achieves the state-of-the-art diarization error rate (DER) of 47.6% on the AVA-AVD benchmark, i.e., an absolute reduction of 23.3% compared to the previous state of the art.

## 2. RELATED WORK: EEND-EDA

EEND-EDA [8] is an end-to-end diarization model that can handle a flexible number of speakers as well as overlapping speech signals. Given a recording, it encodes the audio features into a sequence of audio embeddings  $e_t \in \mathbb{R}^D$ , for  $t \in [1, \dots, T]$ , using stacked Transformer encoders [14] without positional encoding, where  $D$  is the embedding dimension and  $T$  is the total number of audio frames. The encoder is referred to as SA-EEND. Next, in the EDA module, an LSTM encoder encodes the time-shuffled  $e_t$ . Based on the last hidden and cell states of the encoder, an LSTM decoder estimates a flexible number of attractors  $a_s \in \mathbb{R}^D$ ,  $s \in [1, \dots, S]$ , that represent speakers. The estimation process is controlled by a stop flag, representing the complete estimation of all speakers. The speaker activity at time  $t$  for each speaker is obtained by taking the inner product of each attractor with the audio embedding  $e_t$  and applying a sigmoid.

In follow-up work [15], the authors find that the number of output speakers is capped by the maximum found in the pre-training dataset, even if the model is adapted to other datasets with more speakers. This is due to the number of output speakers being limited by the EDA operation. A direct solution would be to pre-train the model on a dataset with more speakers, since the pre-training dataset is often simulated. However, the EDA decoder still needs to estimate many attractors based only on the last hidden and cell states of the EDA encoder. In the next section, we explain our proposed method to generalize EEND-EDA to recordings with more speakers, in addition to simply simulating a matched pre-training dataset.

## 3. PROPOSED METHOD: EEND-EDA-SPKATT

We build upon EEND-EDA [8], proposing an attention EDA module, and jointly training the attractors on the speaker recognition task. Our final model, referred to as EEND-EDA-SpkAtt, is in Fig. 2.

### 3.1. Attention EDA

The original EDA module iteratively estimates an attractor for every speaker in the recording. At each iteration, the EDA LSTM decoder takes as input the previous attractor  $a_{s-1}$ , the previous cell state  $c_{s-1}^d$ , and a zero vector, resulting in a limited capacity to memorize all speakers, and limiting performance when the number of speakers in a recording is large.

Inspired by the attention mechanism in machine translation [16], we propose to use an attention EDA LSTM decoder here, such that the estimation of attractor  $a_s$  is conditioned on a distinct context vector  $z_s$  instead of the zero vector, and  $z_s$  is computed as a weighted sum of the EDA encoder outputs  $h_t^e$ :

$$z_s = \sum_{t=1}^T w_{s,t} h_t^e, \quad (1)$$

$$w_{s,t} = \frac{\exp(f(a_{s-1}, c_{s-1}^d, h_t^e))}{\sum_{\tau=1}^T \exp(f(a_{s-1}, c_{s-1}^d, h_\tau^e))}. \quad (2)$$

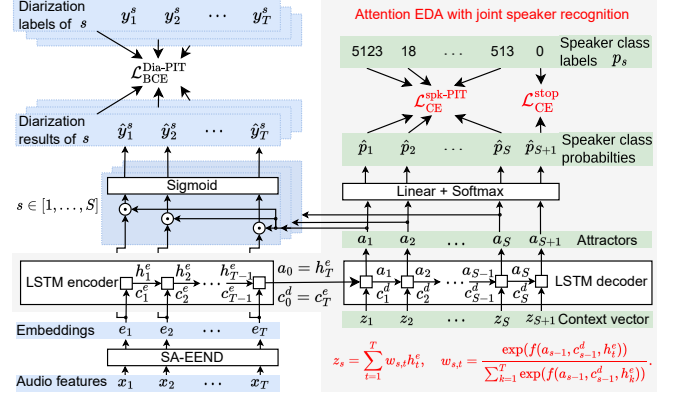


**Fig. 2.** Our proposed EEND-EDA-SpkAtt. We introduce an attention mechanism in EDA to increase its capacity in decoding more speaker attractors, and propose to train the attractors on speaker recognition to improve the attractor representation. The symbol  $\odot$  refers to the inner product. Novel contributions are marked in red.

We parameterize  $f(\cdot)$  as a one-layer feedforward neural network with hyperbolic tangent (tanh) activation. It is worth noting that in EEND-EDA-SpkAtt, we use the SA-EEND with positional encoding, and we do not shuffle the audio embeddings  $e_t$  before passing them to the EDA LSTM encoder, such that the attention mechanism can work properly.

### 3.2. Objective functions for speaker recognition

Besides the final diarization loss, the original EEND-EDA attractors are trained via a binary classification loss in which the attractors iteratively predict whether there are remaining unaccounted-for speakers in the recording, or there are no more speakers. Therefore, the attractors are not explicitly trained to encode speaker information that remains valid across recordings, such as speaker identity. Since each speaker’s activity is conditioned on its attractor, it is understood that a more representative attractor will benefit the diarization task. We are inspired here by speaker extraction approaches in which the speaker extraction is conditioned on an attractor that is jointly trained to recognize the speakers [17–19]. Similarly, we also train the attractors in EEND-EDA-SpkAtt to recognize the speakers, such that the attractors explicitly represent speakers.

We do so by using a softmax layer to transform the attractors  $a_s$  into probability distributions  $\hat{p}_s$  over the speakers in the dataset. During training, we define the ground-truth speaker class labels  $p_s$ ,  $s \in [1, \dots, S]$  using the actual number of speakers  $S$  in a recording, where  $p_s(j)$ ,  $j \in [1, \dots, J]$  is a binary label indicating if the  $s$ -th speaker in the recording is the  $j$ -th speaker in the speaker dataset, and  $J$  denotes the total number of speakers in the training set. We introduce an additional class representing “Not a speaker”, corresponding to  $j = 0$ , and use it as a stop flag, such that the network learns to stop decoding attractors at inference time whenever an attractor falls into this class. The speaker classification objective function for the first  $S$  attractors is defined based on cross-entropy as

$$\mathcal{L}_{\text{CE}}^{\text{Spkr-PT}} = - \arg \min_{\pi \in \mathcal{P}_S} \sum_{s=1}^S \sum_{j=0}^J p_{\pi(s)}(j) \log \hat{p}_s(j), \quad (3)$$

where  $\mathcal{P}_S$  denotes the set of permutations over  $\{1, \dots, S\}$ . We use PIT to find the optimum permutation order between the estimated

attractors and the speaker labels, relying on Sinkhorn’s algorithm (SinkPIT) [20] to avoid the factorial complexity against the number of speakers. At the same time, the  $S + 1$ -th attractor is trained to fall in the “Not a speaker” class, using the objective function defined as

$$\mathcal{L}_{\text{CE}}^{\text{stop}} = - \sum_{j=0}^J p_{S+1}(j) \log \hat{p}_{S+1}(j) = \log \hat{p}_{S+1}(0). \quad (4)$$

### 3.3. Overall objective function

The overall objective function is defined as

$$\mathcal{L}_{\text{all}} = \mathcal{L}_{\text{BCE}}^{\text{Dia-PIT}} + \beta(\mathcal{L}_{\text{CE}}^{\text{spk-PIT}} + \alpha \mathcal{L}_{\text{CE}}^{\text{stop}}), \quad (5)$$

where

$$\mathcal{L}_{\text{BCE}}^{\text{Dia-PIT}} = - \arg \min_{\pi \in \mathcal{P}_S} \sum_{s=1}^S \sum_t (y_t^{\pi(s)} \log(\hat{y}_t) + (1 - y_t^{\pi(s)}) \log(1 - \hat{y}_t)) \quad (6)$$

is the training objective for the diarization task. It is similar to the original EEND-EDA except that the SinkPIT algorithm is used. Different loss terms are balanced using scalar weights  $\alpha$  and  $\beta$ .

## 4. EXPERIMENTAL SETUP

### 4.1. Datasets

The audio-visual AVA-AVD dataset [12] was built upon the AVA-Active Speaker dataset [21], which consists of multilingual movies depicting diverse daily activities, in order to foster the development of diarization methods for challenging conditions. The train, validation, and test sets consist of 243, 54, and 54 videos respectively, and each is 5 minutes long. The histograms of the number of speakers and utterance length are shown in Fig. 1.

Since AVA-AVD is a small dataset, it is a standard practice to pre-train the models on a large simulated dataset first, then fine-tune them on AVA-AVD. Like [12], we use the audio-visual VoxCeleb2 dataset [22], which consists of 1 million YouTube videos from 6112 celebrities, as source material to simulate our pre-training dataset, which we refer to as VoxCeleb2-AVD. In total, we simulate  $2 \times 10^6$ , 500, and 500 recordings for the train, validation, and test sets respectively, and each is 5 minutes long. The test set has disjoint speakers with the train and validation sets.

We strive to simulate VoxCeleb2-AVD as close as possible to AVA-AVD. For each audio recording, we first sample the number of speakers using a normal distribution with mean 8 and standard deviation 2.5, and the minimum (min) and maximum (max) number of speakers are set to 2 and 18, respectively. We select the speakers randomly from the dataset, then sample an utterance randomly from the selected speakers and concatenate all sampled utterances together. The length of each utterance is sampled from a truncated normal distribution with mean 0 and standard deviation 1.5, and with min length of 0.25 s. With probability 0.8, we add silence between the utterances with the silence length sampled from a truncated normal distribution with mean 0.25 and standard deviation 1, and with min length of 0.25 s. With probability 0.2, the following utterance is overlapped with the preceding utterance, with the overlapping duration uniformly sampled between 0.25 s and 2 s, and the max overlapping length is set to the length of the preceding utterance, therefore the dataset has at most two overlapping speakers at any time.

We also randomly sample music and noise clips from the MUSAN dataset [23] and the Freesound Dataset 50k (FSD50K) [24],

and add them to each audio recording. The noise clips are added such that they do not overlap with each other, and about 50% of the length of each audio recording has noise added. The music clips are added similarly to the noise clips. We follow the *cocktail fork* [25] protocol in setting the energy levels between speech, noise, and music in VoxCeleb2-AVD, measuring them by loudness units full-scale (LUFS) [26]. The target LUFS values for speech, music, foreground noise, and background noise are set to  $-17.0$ ,  $-24.0$ ,  $-21.0$ , and  $-29.0$  respectively. For each audio recording, we first sample an average LUFS value for each class uniformly from a range of  $\pm 2.0$  around the corresponding Target LUFS. Then each audio clip added to the audio recording has its individual gain further adjusted by uniformly sampling from a range of  $\pm 1.0$ . We added 0.1 s fade-in and fade-out time for each audio clip.

### 4.2. Implementation details

We train the models on 5-minute recordings. We sample the audio signals at 16 kHz, and obtain 40-dimensional log-Mel-filterbanks features with a 25 milliseconds (ms) frame length and 10 ms frame shift. Each feature is concatenated with those from the previous seven frames and the subsequent seven frames. We sub-sampled the concatenated features by a factor of ten, and the inputs for our model are  $40 \times 15$  dimensional features every 100 ms similarly to [8]. We used SA-EEND with four encoder layers with hidden dimension  $D$  set to 512, feedforward dimension to 1024, drop out to 0.1, and number of heads to 8. The EDA consists of a one-layer LSTM encoder and a one-layer LSTM decoder, which both have hidden size of 512 and drop out of 0.1.

We impose a weight of 5 to the positive class (speaker active) on the diarization loss  $\mathcal{L}_{\text{BCE}}^{\text{Dia-PIT}}$ , to account for class imbalance when there are more speakers involved. We set the scalar weights as  $\alpha = 0.01$  and  $\beta = 0.1 \cdot 0.92^{\text{Epoch}}$ , where  $\text{Epoch}$  is the epoch number, as we empirically found that the speaker recognition loss is important during initial training iterations, but less beneficial as the model converges for diarization. The model is trained using the Adam optimizer with the learning rate schedule proposed in [8, 14] and 10,000 warm-up steps. The batch size is set to 24 on each GPU using gradient accumulation. We train the model on 8 GPUs, thus the effective batch size is  $24 \times 8$ . For both VoxCeleb2-AVD and AVA-AVD, we use the train set to train the model, the validation set to select the diarization threshold, and the test set to report the results.

The training of our proposed EEND-EDA-SpkAtt requires the speaker identity labels in the dataset, and while VoxCeleb2 has such labels, AVA-AVD does not. Since the VoxCeleb2 training set has 5,994 speakers, we can hope to find speakers in that dataset with similar voice characteristics as speakers in AVA-AVD. We thus map the speakers of AVA into the speakers in the VoxCeleb2 training set, based on the L2 distance between their speaker embedding representations extracted using RawNet3 [27], as proxy for their labels.

### 4.3. Baselines

We present the results of three baselines on the AVA-AVD dataset, namely WST [28], VBx [6], and AVR-Net [12]. WST is an audio-visual speaker diarization system that uses audio-visual correlation to help first enroll the speakers and then diarize. VBx is a state-of-the-art audio-only cascaded speaker diarization system that adopts Bayesian clustering; it has two variants, namely VBx-ResNet34 and VBx-ResNet101, that are different in terms of the network lay-

**Table 1.** Results on the simulated VoxCeleb2-AVD dataset. We assign a system number (Sys.) to each model. All systems in this table are only pre-trained on VoxCeleb2-AVD. We report the diarization error rate (DER), which is the sum of missed speech (MS), false alarm speech (FA), and speaker error (SPKE). We also report the Jaccard error rate (JER). The lower the better for all metrics, while bold values represent best results. All results reported in this paper are with a collar of 0.25 s [30].

Sys.	Model	MS	FA	SPKE	DER	JER
6	EEND-EDA [8]	17.4	9.1	18.9	45.4	66.7
8	EEND-EDA-SpkAtt	15.8	6.7	18.2	<b>40.8</b>	<b>62.8</b>
10	EEND-EDA-Spk	25.1	6.4	17.6	49.1	71.2
12	EEND-EDA-Att	14.6	8.6	20.8	43.9	66.6

ers extracting x-vectors [2]. AVR-Net is an audio-visual cascaded speaker diarization system that is built upon VBx-ResNet34 and TalkNet [29]. We report the results published in [12] for the above-mentioned baselines, which are all pre-trained on the VoxCeleb2 dataset first and fine-tuned on AVA-AVD.

## 5. RESULTS

### 5.1. Results on VoxCeleb2-AVD

In Table 1, we present the results of the baseline EEND-EDA and our EEND-EDA-SpkAtt trained and evaluated on the simulated VoxCeleb2-AVD dataset. Our EEND-EDA-SpkAtt achieves the best DER and JER. Further decomposing DER, ours is better for all its submetrics: MS, FA, and SPKE.

We also present two ablation studies of our EEND-EDA-SpkAtt. EEND-EDA-Spk (system 10) is trained with our speaker recognition loss, but without the attention mechanism. System 10 performs badly in terms of DER and JER due to higher MS; this is probably because the vanilla EDA has limited capacity in decoding attractors that are representative of speakers, thus the speaker loss adversely affects the model training. EEND-EDA-Att (system 12) has the attention mechanism in EDA, but is not trained with our speaker recognition loss. System 12 outperforms system 6 in DER, but is not better than system 8 except for the MS submetric.

### 5.2. Results on AVA-AVD benchmark

In Table 2, we compare our EEND-EDA-SpkAtt with baselines on the AVA-AVD benchmark. According to [12], systems 2-4 use the same VAD, thus obtaining the same MS and FA. The previous state of the art is VBx-ResNet101 in system 3, which reports a DER of 70.9%. Without pre-training, EEND-EDA in system 5 performs badly with a DER of 96.4%. Systems 6-9 are pre-trained on our VoxCeleb2-AVD, and they all outperform the baselines by a wide margin in terms of DER, with our EEND-EDA-SpkAtt achieving the best DER of 47.6% and JER of 76.4%. It is worth mentioning that our EEND-EDA-SpkAtt is an audio-only model, but still outperforms the audio-visual baselines, i.e., the WST and AVR-Net models, by a wide margin.

We also perform ablation studies with EEND-EDA-Spk and EEND-EDA-Att on the AVA-AVD benchmark. Similarly to the results on VoxCeleb2-AVD in Table 1, EEND-EDA-Spk in systems 10 and 11 performs badly compared to the vanilla EEND-EDA model,

**Table 2.** Results on the AVA-AVD benchmark. PT indicates the model is either pre-trained on a VoxCeleb2-based dataset (systems 1-4) as in [12], or is pre-trained on our VoxCeleb2-AVD (systems 6-15), while FT indicates the model is fine-tuned on AVA-AVD. \*Systems 14 and 15 use the ground-truth number of speakers at inference.

Sys.	Model	PT	FT	MS	FA	SPKE	DER	JER
1	WST [28]			11.6	40.6	36.1	88.4	-
2	VBx-ResNet34 [6]	✓	✓	8.7	44.6	35.3	88.5	-
3	VBx-ResNet101 [6]			8.7	44.6	17.6	70.9	-
4	AVR-Net [12]			8.7	44.6	20.1	73.3	-
5	EEND-EDA [8]	✗	✓	46.6	27.3	22.6	96.4	94.7
6	EEND-EDA [8]	✓	✗	24.2	2.8	24.4	51.4	83.5
7	EEND-EDA [8]	✓	✓	28.5	5.3	15.1	48.9	78.5
8	EEND-EDA-SpkAtt	✓	✗	22.8	6.8	20.8	50.4	80.5
9	EEND-EDA-SpkAtt	✓	✓	25.0	5.6	17.0	<b>47.6</b>	<b>76.4</b>
10	EEND-EDA-Spk	✗		29.8	4.0	21.8	55.6	84.5
11	EEND-EDA-Spk	✓	✓	35.4	3.3	16.4	55.1	82.7
12	EEND-EDA-Att	✗		28.3	3.6	20.1	52.1	82.2
13	EEND-EDA-Att	✓		38.2	1.8	14.2	54.2	82.0
14	EEND-EDA* [8]	✓	✓	28.7	4.7	15.3	48.7	78.5
15	EEND-EDA-SpkAtt*	✓	✓	23.2	7.8	16.7	47.7	74.3

mostly due to worse MS. EEND-EDA-Att also does not generalize well on the AVA-AVD benchmark. Therefore, we come to the conclusion that the speaker recognition loss and the attention mechanism only help if they are used together, which is reasonable since the attention mechanism increases EDA’s capacity in estimating more speaker attractors to work with the speaker recognition loss, while the speaker recognition loss regularizes the attention module.

### 5.3. Results on AVA-AVD with oracle speaker counting

We also present systems 14 and 15 in Table 2 as upper-bound analysis, to study the effects of estimating the number of speakers in diarization performance. For baseline EEND-EDA, system 14 is the same as system 7, except that the former uses the ground-truth number of speakers at inference. We can see that they have similar DER and JER, this could be a reason for the trade-offs between different components in DER and JER. For our EEND-EDA-SpkAtt, system 15 is the same as system 9, except that the former uses the ground-truth number of speakers at inference. Both have similar DER, but system 9 is lagging behind system 15 by 2% in terms of JER. We observe that our proposed system 9 typically underestimates the number of speakers, nevertheless, system 9 still achieves the best DER and JER, credited to our better attractor representation. We plan to address the gap in speaker number estimation in our future work.

## 6. CONCLUSION

In this work, we presented the end-to-end neural speaker diarization model EEND-EDA-SpkAtt, to deal with in-the-wild recordings. It features an attention mechanism to increase the capacity of the attractor estimation module, as well as a speaker recognition loss to improve the attractor representation. By pre-training EEND-EDA-SpkAtt on our carefully-simulated pre-training dataset VoxCeleb2-AVD, we outperform the state of the art by a wide margin.

## 7. REFERENCES

- [1] Z. Pan, Z. Luo, J. Yang, and H. Li, “Multi-modal attention for speech emotion recognition,” in *Proc. Interspeech*, 2020, pp. 364–368.
- [2] D. Snyder, D. Garcia-Romero, G. Sell, D. Povey, and S. Khudanpur, “X-vectors: Robust DNN embeddings for speaker recognition,” in *Proc. ICASSP*, 2018, pp. 5329–5333.
- [3] X. Qian, M. Madhavi, Z. Pan, J. Wang, and H. Li, “Multi-target DoA estimation with an audio-visual fusion mechanism,” in *Proc. ICASSP*, 2021, pp. 4280–4284.
- [4] Z. Pan, M. Ge, and H. Li, “A hybrid continuity loss to reduce over-suppression for time-domain target speaker extraction,” in *Proc. Interspeech*, 2022, pp. 1786–1790.
- [5] T. J. Park, N. Kanda, D. Dimitriadis, K. J. Han, S. Watanabe, and S. Narayanan, “A review of speaker diarization: Recent advances with deep learning,” *Comput. Speech Lang.*, vol. 72, p. 101317, 2022.
- [6] F. Landini, J. Profant, M. Diez, and L. Burget, “Bayesian HMM clustering of x-vector sequences (VBx) in speaker diarization: Theory, implementation and analysis on standard tasks,” *Comput. Speech Lang.*, vol. 71, p. 101254, 2022.
- [7] Y. Fujita, N. Kanda, S. Horiguchi, K. Nagamatsu, and S. Watanabe, “End-to-end neural speaker diarization with permutation-free objectives,” in *Proc. Interspeech*, 2019, pp. 4300–4304.
- [8] S. Horiguchi, Y. Fujita, S. Watanabe, Y. Xue, and K. Nagamatsu, “End-to-end speaker diarization for an unknown number of speakers with encoder-decoder based attractors,” in *Proc. Interspeech*, 2020, pp. 269–273.
- [9] S. Horiguchi, Y. Fujita, S. Watanabe, Y. Xue, and P. García, “Encoder-decoder based attractors for end-to-end neural diarization,” *IEEE/ACM Trans. Audio, Speech, Lang. Process.*, vol. 30, pp. 1493–1507, 2022.
- [10] Y. Isik, J. Le Roux, Z. Chen, S. Watanabe, and J. R. Hershey, “Single-channel multi-speaker separation using deep clustering,” in *Proc. Interspeech*, 2016, pp. 545–549.
- [11] D. Yu, M. Kolbæk, Z.-H. Tan, and J. Jensen, “Permutation invariant training of deep models for speaker-independent multi-talker speech separation,” in *Proc. ICASSP*, 2017, pp. 241–245.
- [12] E. Z. Xu, Z. Song, C. Feng, M. Ye, and M. Z. Shou, “AVA-AVD: Audio-visual speaker diarization in the wild,” in *Proc. ACM Multimedia*, 2022.
- [13] N. Ryant, K. Church, C. Cieri, J. Du, S. Ganapathy, and M. Liberman, “Third DIHARD challenge evaluation plan,” *arXiv preprint arXiv:2006.05815*, 2020.
- [14] A. Vaswani, N. Shazeer, N. Parmar, J. Uszkoreit, L. Jones, A. N. Gomez, Ł. Kaiser, and I. Polosukhin, “Attention is all you need,” *Proc. NeurIPS*, vol. 30, 2017.
- [15] S. Horiguchi, S. Watanabe, P. García, Y. Xue, Y. Takashima, and Y. Kawaguchi, “Towards neural diarization for unlimited numbers of speakers using global and local attractors,” in *Proc. ASRU*, 2021, pp. 98–105.
- [16] D. Bahdanau, K. Cho, and Y. Bengio, “Neural machine translation by jointly learning to align and translate,” *Proc. ICLR*, 2014.
- [17] K. Žmolíková, M. Delcroix, K. Kinoshita, T. Higuchi, A. Ogawa, and T. Nakatani, “Learning speaker representation for neural network based multichannel speaker extraction,” in *Proc. ASRU*, 2017, pp. 8–15.
- [18] Z. Pan, R. Tao, C. Xu, and H. Li, “MuSE: Multi-modal target speaker extraction with visual cues,” in *Proc. ICASSP*, 2021, pp. 6678–6682.
- [19] —, “Selective listening by synchronizing speech with lips,” *IEEE/ACM Trans. Audio, Speech, Lang. Process.*, vol. 30, pp. 1650–1664, 2022.
- [20] H. Tachibana, “Towards listening to 10 people simultaneously: An efficient permutation invariant training of audio source separation using Sinkhorn’s algorithm,” in *Proc. ICASSP*, 2021, pp. 491–495.
- [21] J. Roth, S. Chaudhuri, O. Klejch, R. Marvin, A. Gallagher, L. Kaver, S. Ramaswamy, A. Stopczynski, C. Schmid, Z. Xi, *et al.*, “AVA active speaker: An audio-visual dataset for active speaker detection,” in *Proc. ICASSP*, 2020, pp. 4492–4496.
- [22] J. S. Chung, A. Nagrani, and A. Zisserman, “VoxCeleb2: Deep speaker recognition,” in *Proc. Interspeech*, 2018, pp. 1086–1090.
- [23] D. Snyder, G. Chen, and D. Povey, “MUSAN: A music, speech, and noise corpus,” *arXiv preprint arXiv:1510.08484*, 2015.
- [24] E. Fonseca, X. Favory, J. Pons, F. Font, and X. Serra, “FSD50K: An open dataset of human-labeled sound events,” *IEEE/ACM Trans. Audio, Speech, Lang. Process.*, vol. 30, pp. 829–852, 2021.
- [25] D. Petermann, G. Wichern, Z.-Q. Wang, and J. Le Roux, “The cocktail fork problem: Three-stem audio separation for real-world soundtracks,” in *Proc. ICASSP*, 2022, pp. 526–530.
- [26] E. Grimm, R. Van Everdingen, and M. Schöpping, “Toward a recommendation for a European standard of peak and LKFS loudness levels,” *SMPTE Motion Imaging J.*, vol. 119, no. 3, pp. 28–34, 2010.
- [27] J.-W. Jung, Y. J. Kim, H.-S. Heo, B.-J. Lee, Y. Kwon, and J. S. Chung, “Pushing the limits of raw waveform speaker recognition,” in *Proc. Interspeech*, 2022.
- [28] J. S. Chung, B.-J. Lee, and I. Han, “Who said that?: Audio-visual speaker diarisation of real-world meetings,” in *Proc. Interspeech*, 2019, pp. 371–375.
- [29] R. Tao, Z. Pan, R. K. Das, X. Qian, M. Z. Shou, and H. Li, “Is someone speaking? Exploring long-term temporal features for audio-visual active speaker detection,” in *Proc. ACM Multimedia*, 2021, pp. 3927–3935.
- [30] D. Istrate, C. Fredouille, S. Meignier, L. Besacier, and J. F. Bonastre, “NIST RT’05S evaluation: Pre-processing techniques and speaker diarization on multiple microphone meetings,” in *Int. Workshop Mach. Learn. Multimodal Interact.*, 2005, pp. 428–439.